

Rotating Objects via In-Hand Pivoting using Vision, Force and Touch

Shiyu Xu¹, Tianyuan Liu¹, Michael Wong¹, Dana Kulić¹, Akansel Cosgun²

Abstract—We propose a robotic manipulation system that can pivot objects on a surface using vision, wrist force and tactile sensing. We aim to control the rotation of an object around the grip point of a parallel gripper by allowing rotational slip, while maintaining a desired wrist force profile. Our approach runs an end-effector position controller and a gripper width controller concurrently in a closed loop. The position controller maintains a desired force using vision and wrist force. The gripper controller uses tactile sensing to keep the grip firm enough to prevent translational slip, but loose enough to induce rotational slip. Our sensor-based control approach relies on matching a desired force profile derived from object dimensions and weight and vision-based monitoring of the object pose. The gripper controller uses tactile sensors to detect and prevent translational slip by tightening the grip when needed. Experimental results where the robot was tasked with rotating cuboid objects 90 degrees show that the multi-modal pivoting approach was able to rotate the objects without causing lift or slip, and was more energy-efficient compared to using a single sensor modality and to pick-and-place. While our work demonstrated the benefit of multi-modal sensing for the pivoting task, further work is needed to generalize our approach to any given object.

I. INTRODUCTION

Robotic manipulation can be prehensile or non-prehensile. Prehensile manipulation involves capturing the object (e.g., via grasping) and requires achieving stable control over the grasped object. During object transport, prehensile manipulation requires the object to be lifted and held stably in the grasp. Non-prehensile manipulation, on the other hand, is a type of manipulation where objects are manipulated without grasping them. Non-prehensile manipulation allows a robot to perform a wider range of tasks than prehensile manipulation and can be more energy-efficient than prehensile manipulation because it does not require the robot to use as much force to move the object. In this study, we focus on performing pivoting actions on objects grasped by a parallel gripper. As shown in Fig.1, this action takes an interesting middle ground between non-prehensile and prehensile manipulation. On the one hand, it requires the object to be grasped and gives the robot more stable control over the pose of the object. On the other hand, the action does not require the target object to be lifted off the surface on which it is placed. In the example shown in Fig.1, to avoid the need to turn the gripper along with the box, which introduces additional kinematic constraints on the robot, the box needs to rotate around the grasp point. These actions require much less effort than performing a full pick and place [1], bringing much of the benefits non-prehensile techniques in simplicity and a reduction in the amount of work done. With less force exerted, this approach may even allow

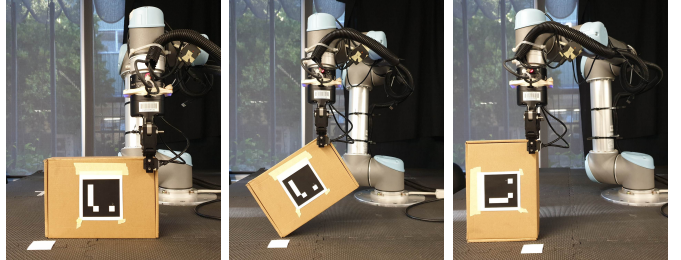


Fig. 1: The robot pivots a box by 90 degrees in one motion while maintaining contact between the box and the surface. The end effector position is controlled using vision and wrist force sensing while the gripper width is controlled using tactile sensing.

the manipulation of objects heavier than the maximum payload of a robot [2].

This study investigates reorienting an object grasped by a parallel gripper using pivoting actions. To achieve in-hand manipulation with a simple parallel gripper with no dexterous capabilities, we make use of extrinsic environmental factors [3]. Specifically, once the object is grasped, gravity is used to induce slip and rotate the object in-hand when lifting the gripper. Meanwhile, friction with the surface provides an opposing force to fully pivot the object. Thus, to allow this friction, the object must also be kept in contact with the surface during the motion.

Enabling slip in the grasp of the object is a non-trivial problem. To achieve the desired slip, the appropriate gripper finger width needs to be chosen in accordance to the properties of the object. As the object and its center of mass (CoM) move during the pivot, the dynamic effects should also be considered.

To gain better insight into the forces that can induce in-hand slip, we follow other works on slip detection [4]–[6] in differentiating slip into two types, rotational slip and translational or linear slip. As shown in Fig.2, rotational slip is where the object is allowed to rotate while remaining grasped, with its center of rotation at the grasp point and remaining in place as the object moves. Translational or linear slip involves the object moving away from the original grasping point. These two types of slip can occur on their own or simultaneously. For an in-hand pivoting task, the goal is to avoid translational slip, while allowing rotational slip [7].

Similarly, the trajectory of the pivoting motion also needs to be adjusted to ensure the objects remain in contact with the surface. Visual information may be used to determine the object's pose, but contact with the surface may be challenging to estimate visually. On the other hand, force data can be used to derive whether the object is lifted by the robot, but otherwise would provide little information about the object's pose.

We propose using multi-modal sensing in closed-loop con-

¹Monash University, Australia

²Deakin University, Australia

This work was supported in part by D. Kulić's Australian Research Council Future Fellowship (FT200100761).

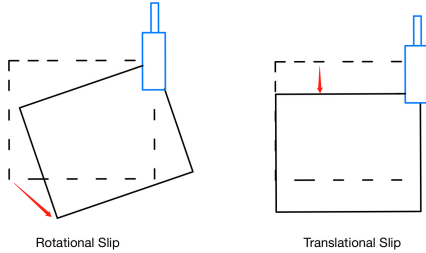


Fig. 2: The two types of slip. The dotted outline describes the original position, and solid shape is the position after slip. The blue object is the gripper fingers.

trol that can adjust both the robot arm trajectory and the gripper width to complete a pivoting action. The object state will be continuously detected through force/torque data at the parallel fingers and wrist of the gripper, as well as visual information from an RGB-D camera. Pivoting of the grasped object will then be achieved through motion planning with the arm's end-effector coupled with a position controller, while slip will be managed by adjusting the gripper width. Overall, the main contributions of this study include:

- A vision and force-based position controller for the arm trajectory that integrates an analytical force profile and object pose information
- A tactile sensor-based gripper width controller for parallel grippers that tightens based on detected slip
- Experiments on a real robot that validate the effectiveness of multi-modal sensing for the pivoting task

II. RELATED WORKS

Pivoting provides an alternative to pick-and-place methods for reorienting the pose of an object. Although a significant advantage of the pivoting motion is the ability to extend manipulation to reorienting heavy, large and/or long objects [8]–[11] that cannot be picked up by robot, we consider pivoting smaller and lighter objects as a proof-of-concept for such use cases.

Previous works focus on in-hand pivoting where the object is held in air [7], [12] while others target pivoting using a surface to support the motion [8]–[11]. For our purposes, we will focus on pivoting with the assistance of a surface.

To achieve pivoting, planning based approaches are frequently adopted [8], [9], [11], [13], [14]. Closed loop control is also common, such as Shi *et al.* who implemented impedance and admittance control to optimise the force planner they designed for their aerial robot [10]. Machine learning methods are also used to control robot behaviour using complex input data [7], [12]. Our solution aims at a learning-free control algorithm for the gripper width as well as end effector position during a pre-planned pivoting motion.

A. Contact Control

Adopting a purely open loop approach can often be limiting as the robot only considers the environment's initial states and is unaware how its interactions influence them [15]. In terms of the pivoting action, the motion of the robot needs to be updated

based on the object's contact with the surface to induce friction and complete a full pivot.

For similar tasks, force and torque data is often used to estimate the state of the robot held object's contact with its surroundings. Ma *et al.* detected extrinsic contact between a grasped object and the environment using tactile sensors mounted to a parallel gripper [16]. Molchanov *et al.* used a data-driven approach, training machine learning models with tactile data to perform regression and classification for the presence and location of contact between object and environment [17]. Doshi *et al.* used force/torque data to estimate how a wrench applied to an object would affect its motion using a contact model [18]. Hogan *et al.* used high-resolution tactile sensors to localise the pose of held object and estimate contact and slip status. Both [18] and [19] also developed and experimentally tested closed loop controllers for manipulation.

Vision inputs are also used to compliment tactile data. Yu *et al.* trained a learning model with visually detected pose estimates for a object of known geometry, as well as tactile data from a wrist force/torque sensor and robot encoders [20]. The model was used to detect the contact arrangement of a held object, and achieved more accurate estimates than using vision alone.

We take a multi-modal approach to maintain extrinsic contact, using vision-based pose estimation and force-based position control compared with a simpler vision-only method.

B. Slip Control

To achieve an angled pivoting position with relatively simple motions, gravity is used to induce slippage at the fingertips of the gripper, allowing change of pose without having to regrasp an object. The application of control methods, as previously discussed, can also greatly improve the capability for the system to maintain desired slip during dynamic motion. To detect slip, tactile sensing at the contact with the object is often used [21]. Costanzo *et al.*'s line of work investigated, separately, the prevention of both rotational and translational slip, as well as enabling rotation while preventing linear slip [4], [22], [23]. They input force and torque data into an analytical friction model to estimate slippage, and develop a controller that prevents undesired slip with minimum force [23]. Wang *et al.* similarly used a friction model to develop a slip estimation algorithm and a gripper controller [24]. Data-based approaches are also prominent, with Toskov *et al.* and Chen *et al.* both training machine learning models to perform slip under gravity, with Toskov *et al.* focusing on rotational slip [7] and Chen *et al.* focusing on translational slip [25]. While existing works predominantly pivot the objects in the air [7], [23]–[25], we will attempt to detect and control slip while maintaining contact between the object and the surface it rests on, which allows the robot to reorient objects without needing to pick up and lift them, reducing effort required.

III. APPROACH

For simplicity, we will focus on a box-shaped object with only one out of three dimensions that is within the gripper's

graspable width. This is because it'd be easier to design an algorithm for a box as opposed to an irregularly shaped object.

The pivoting task is divided into three sub-tasks. The first section covers visual object pose detection where the 6D pose of the box is estimated. The second part contains the generation of the grasp pose, which is be placed on a point along the top edge of the box based on a user input. Finally, closed loop gripper width control is used to grasp the object, and further regulates slip during the pivot motion. A force-based end-effector position controller is also used to amend a pre-planned end-effector trajectory, aiming to maintain contact between the grasped box and the surface. The control loop runs until robot is able to complete the pivoting task, or when all waypoints of the pre-planned path has been executed. This overall structure of the system is illustrated in Fig.3.

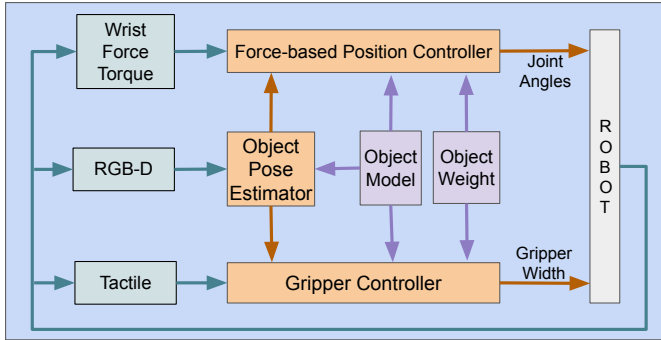


Fig. 3: System diagram

A. Object Pose Estimation

An RGB-D side camera is used to detect the ArUco marker placed in the center of the largest surface of the box. Based on this marker detection as well as the box dimensions, the box pose can be inferred by offsetting the marker's pose by half of the box's respective dimension. The 6D pose of the box's axis of origin, is defined at its centre point with an orientation that aligns the axes so that they are parallel with the length, width and height of the box.

B. Grasp Pose Synthesis

From the box's pose, a feasible grasp pose will be generated using the known dimensions of the box. The gripper will grasp the box such that the gripper is perpendicular to the table surface, i.e. the gripper is pointing down into the table. The grasp pose is also positioned ensuring that all pillars of the tactile sensors would make contact with the box. Given that there is only one graspable dimension, the robot can only grasp along one surface of the box. The user is able to input a number to choose which end of the box should be grasped.

The placement of the grasp pose on the top corner of the box prevents the box from being stopped by the gripper palm during the pivoting motion, and allows it to fit through the gap between the fingers. The grasp point relative to the box, as well as the orientation of the gripper, is maintained during the pivoting action. For a given grasp point, the pivot direction is always chosen such that the grasp point and pivot point are

on opposite sides of the box. This is demonstrated in Fig.1.

C. Closed Loop Control

To successfully pivot the box we employ a robot end-effector position controller and a gripper controller. These controllers will adjust both the robot end-effector trajectory and the gripper width respectively throughout the pivoting motion.

Initial Gripper Width: Determining an adequately loose grip width is essential to enabling rotational slip to allow the box to rotate in-hand. To grasp the box, an initial grip width is first determined using tactile sensors and the graspable dimension of the box. This is calculated by dividing the length of the graspable dimension by the distance between the two tactile sensors. Additionally, to ensure that the gripper does not experience translational slip initially, the static friction force applied by the gripper must be greater than the force of the box on the gripper at the point where the robot pivots the box $d\theta$.

$$F_{\text{static}} = \mu_s F_N \quad (1)$$

$$F_{\text{static}} > F(d\theta) \quad (2)$$

The force at $d\theta$ is taken as this is the instantaneous force on the gripper as the robot starts pivoting the box. The normal reaction force is found by the tactile sensor reading. This will ensure that the gripper is tight enough to start pivoting the box. Until this condition is met, the gripper will continue to close itself.

Force-based Position Controller: The robot force-based position controller controls and updates the arm's trajectory throughout the pivoting motion. This controller utilises the force/torque wrist sensor which provides force readings, and the RGB side camera which detects and estimates the box's rotation angle as the robot pivots the box.

We represent a complete pivoting motion with the pivot point of the object remaining in contact with the surface by an ideal force profile. This profile is derived through analysis of the forces applied to the object during pivoting. It varies with respect to the progress of the pivot, as indicated by the angle of rotation. The controller will then maintain contact by tracking this profile. The force exerted by the robot is controlled by applying a vertical offset to a pre-planned arc trajectory for the end-effector.

Initially, a Cartesian path consisting of 50 waypoints is generated using the MoveIt motion planning framework, that instructs the robot to move with an arc trajectory parameterised by the box's dimensions. 50 waypoints are used as it strikes a balance between time taken to complete the movement as well as maintaining the trajectory resolution to keep the arc shape, as a circular arc with radius as the distance between the grasp point and the pivot point. For a box grasped at the top corner, the radius would become its diagonal, as seen in Fig.4.

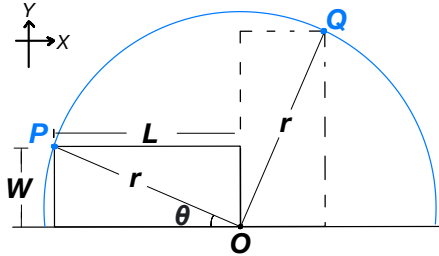


Fig. 4: Path Analysis: the box is pivoting from the solid line position to dashed line position, O is the pivoting center, P is the grasp point at the beginning of the pivoting and Q is the corresponding point of P after pivoting.

To pivot the box from point P to point Q , the position of that point's trajectory is:

$$\text{Position}_x = L - r \cdot \cos(\theta) \quad (3)$$

$$\text{Position}_y = r \cdot \sin(\theta) \quad (4)$$

where L is the length of the box, the arc radius r is the diagonal of the box and θ can be calculated from the box's dimension.

The analytical force profile was derived assuming equilibrium conditions during the pivot action, corresponding to a stationary configuration, or a constant speed rotation. In such a case, as illustrated in Fig.5, torque applied on the box by the gravitational force F_g , with the centre of mass assumed to be at the centre of the box, is balanced by the forces applied to it from the pivoting motion F_p .

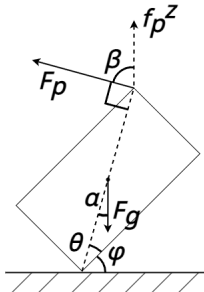


Fig. 5: Free-body diagram of a pivoting box under equilibrium conditions

The force that would be measured by the wrist sensor in the vertical (z) direction is derived as the the vertical component of pivoting force F_p , f_p^z :

$$f_p^z = \frac{F_g \sin(\alpha) \cos(\beta)}{2} \quad (5)$$

The above equation can then be expressed with respect to the angle of rotation of the box, ϕ , and specific properties of the box, including the angle between its base and diagonal, θ , its mass m , as well as the gravitational constant g :

$$f_p^z = \frac{m g \sin\left(\frac{\pi}{2} - \phi - \theta\right) \cos(\phi + \theta)}{2} \quad (6)$$

From empirical tests, the relationship between the height that the gripper lifts the box up to and the force measured by the wrist sensor during surface-contact pivoting was found to be roughly linear. Thus, to control the force applied to the box, a vertical offset is applied to the trajectory for every waypoint.

Using the above information, the position controller is implemented, and described in Alg.1. At each waypoint, the ideal force f_{ideal} is predicted using the rotation angle of the box, estimated using vision. The measured force f_{real} is then compared to the ideal force to produce an error, and accumulated in $error_{acc}$. The vertical offset that should be applied is then calculated from the force error using a Proportional-Integral (PI) control scheme. A proportional constant K_p is applied to the instantaneous error, and an integral constant K_i is applied to the accumulated error. Both constants are empirically tuned. The offset is applied to all waypoints, and adjusted incrementally during each iteration. This aims to maintain the offset that minimises the error between the two force values. The pre-planned waypoint is updated by applying this offset to the vertical dimension, and re-planned so that the robot will move in accordance to the adjustment. If at any point the rotation angle is estimated to be greater than or equal to 90° , it is assumed that the pivot is complete and the program will terminate.

Algorithm 1 Trajectory force-based position controller, using z as the vertical dimension

```

offset ← 0
erroracc ← 0
for waypoint in trajectory do
    φ ← vision_detection
    freal ← force_torque_sensor
    fideal ← ideal_force_profile(φ)
    if φ < 90° then
        error ← |fideal - freal|
        erroracc ← erroracc + error
        offset ← offset + Kp × error + Ki × erroracc
        waypoint.z ← waypoint.z + offset
        move_robot(waypoint)
    else
        break
    end if
end for

```

Due to the assumption of equilibrium and the replanning of waypoints for each iteration, the robot is required to pause momentarily before each consecutive movement to the next waypoint. This causes a discontinuous, slow motion that becomes slower with more waypoints.

Gripper Controller: The slip of the object will be controlled to perform the pivoting movement. We first estimate the slip type by detecting either translational or rotational slip. We ignore the no slip case as for boxes that are heavier than a certain weight, the gripper cannot grasp the box without experiencing rotational or translational slip. During the process of pivoting, the desired slip is rotational slip and translational



Fig. 6: The cardboard boxes used for pivoting. Based on their shapes, the boxes are referred to as, from left to right: Small box (18x11x4cm, 1.27kg), Large box (23x16x5cm, 0.88kg), Long box (28x12x5cm, 1.72kg)

slip should be avoided.

To detect the type of slip, the 3D displacement data and contact estimation from the tactile sensors on the gripper fingers is used. We specifically utilise displacement in the direction parallel to the force of gravity on the box. If there is translational slip, the box will move in that direction relative to the tactile sensor. Again, we focus on the vertical dimension as gravity is the major factor causing slip. When all pillars that are detected to be in contact with the box show displacement values in the same direction (i.e. their displacement values share the same sign), the box is labelled to be in translational slip. This is in contrast to when the box undergoes rotational slip, where pillars would be displaced in different directions with opposing signs in displacement values, as the centre of rotation is roughly at the centre of the sensor.

If the tactile sensors detect translational slip, the gripper width will close slightly, whereas if the tactile sensors detect rotational slip, then the gripper width is unaltered. The gripper will also loosen its grip if at least one of the pillars experience a displacement of over 8mm, to prevent damage to the sensors and the box.

IV. EXPERIMENTS

A. Setup

The proposed pivoting system was tested using a single UR5 robot arm with the Robotiq 2F-85 gripper attached to end of the robot arm. The end effector also has a FT-300 Force/Torque sensor attached. The fingers of the gripper have two Contactile PapillArray 3x3 tactile sensor arrays attached, capable of measuring 3D displacement, force, and torque [26]. The camera used for vision is the Intel RealSense D435i, placed to the side of the robot. The hardware setup is shown in Fig 7.

Objects that will be used for experimentation are cardboard boxes with varying dimensions, shown in Fig.6. Their mass and mass distributions are adjustable by adding iron weights inside.

B. Procedure

A series of experiments are designed to verify the validity of our approach. These experiments will represent increasing levels of difficulty for the robot. The goal of all four experiments is to complete a 90° rotation of the box without lifting it off the surface or letting the box slip out of the gripper's grasp. A simple pick-and-place method will also be performed as a baseline. We compare five different methods,

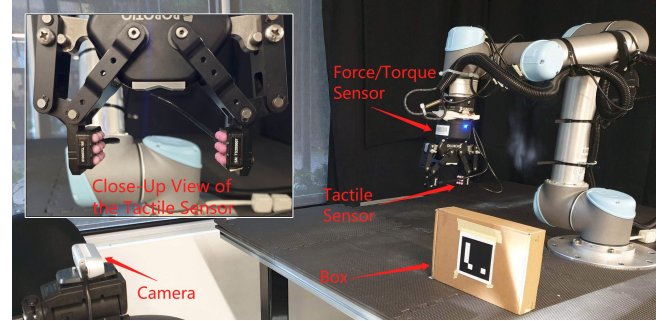


Fig. 7: Experimental Setup

including those introduced in Section III-C, and subject each to four different conditions. Each applicable combination was repeated 10 times for each of the three boxes. The methods and conditions are described below.

C. Methods

Pick&Place: The robot first lifts up the box completely and then rotates it in the air by 90°, and completes pivoting after lowering it down. The gripper is set to close as hard as possible. The lifted height before pivoting and the lowered down height after pivoting is set just high enough so that the robot can complete pivoting without hitting the surface to represent the lowest effort situation using this method.

Open Loop: No controllers are used under this method. The gripper is set to close as hard as possible. The arm's trajectory planned is an ideal arc based on the box's dimensions.

Vision: A vision-based controller is used as a comparison to the force-based position controller. The gripper is set to close as hard as possible. Similar to the force-based position controller, the arm's trajectory is planned as an ideal arc based on the box's dimensions. However, the vertical offset is calculated from the estimated height of the box from the surface, rather than error from the force profile.

Gripper: Only the gripper controller is used, both to grasp the object and to control slip during pivoting. The arm's trajectory is planned as an ideal arc, not updated during the movement.

Force: Only the force-based position controller is used. The gripper is set to close as hard as possible. The arm's trajectory planned is an ideal arc and updated during the movement using the error between measured force and predicted force.

Force+Gripper+Vision: All three sensors are used in this method. The gripper controller is used to grasp the object and control slip. Vision is used to track the rotation angle between the surface and the box's lowest edge for force calculation purpose. The arm's trajectory is planned as an arc at the beginning and updated during the movement by the force-based position controller, and the gripper width is updated by gripper controller.

D. Independent Variables

- 1) **Pivoting types:** The robot performs two types of pivoting. It either pivots a box from standing on its longer edge to standing on its shorter edge, or from its shorter edge to its longer edge.

2) **Noise:** A 5cm noise value for the base dimension of the box can be added, causing the arc trajectory to have a larger radius. No noise represents the ideal arc trajectory.

E. Evaluation Metrics

To assess the performance of the robot in each experiment, five quantitative measures are established:

- **Success Rate (%)**: The percentage of all attempts where the robot fully completes the 90° rotation.
- **Slip Off Rate (%)**: The percentage of all attempts where the box slips off from the gripper during the movement.
- **Lift Up Rate (%)**: The percentage of all attempts where the box is lifted off the surface during the movement, regardless of whether contact was re-established later during the motion.
- **Time Taken (s)**: The total complete time it takes the robot to move the object from the start to end position as soon as the goal pose is known.
- **Work (Joules)**: The amount of both translational work and rotational work done applied by the robot on the object to move the object from the start to goal pose.

A pivot action is considered as a failure when the robot cannot complete the rotation. Lift up and slip off rates are used to distinguish between perfect success (i.e. neither leaving nor being pushed too hard into the surface) and conditional success, which is less efficient in terms of effort and has a higher risk in damaging the manipulated object or the environment.

F. Results

The detailed results for all experiments can be found in Table I - III, with the aggregate results presented in Table IV. The combined controller approach achieves 100% rate with 0 lift up and 0 slip off rates. This approach also has the least work consumption among all approaches while the pick&place method required the highest work done. However, it lags behind other methods in terms of completion time. Instead, the open loop approach requires the least time to complete the movement.

V. DISCUSSION

A. Highest Performance and Robustness

Performance: The combined approach of vision, force-based position and gripper control had the highest success rate and lowest work done among all approaches. It was able to adjust both the gripper width and the moving trajectory so that the object will not be lifted off the ground. However, the long completion time of 27.4 seconds on average is the disadvantage of our approach. As discussed in Section III-C, this is due to the replanning of each subsequent end-effector waypoint when applying the control offset, which requires more time than other approaches. The fastest approach was the open loop method with an average completion time of 10.3 seconds, as it only plans once for the entire trajectory. On the other hand, this also indicates that the pivoting action is capable of faster completion than the traditional pick-and-

place method (16.8 seconds on average). If a more responsive control methodology such as pure joint velocity control without planning was implemented, the closed loop solution may also achieve speeds approaching the open loop method.

The lift and slip rates indicate the importance of the gripper controller. For methods that do not use gripper controller, closing the gripper as hard as possible avoids translational slip. This is reflected in the very low slip rate across all methods, even when the boxes have been lifted off the surface. Meanwhile, without the gripper controller, rotational slip could not be achieved consistently, and was prone to influences by other factors such as the box's mass, shape and mass distribution. Without rotating in the gripper, the pivot point would lose contact with the surface as the box cannot maintain a pose that keeps its diagonal in line with the radius of the trajectory. This corresponds to higher lift rates for most cases compared to methods with gripper controller.

Robustness: For the purpose of testing robustness, noise is intentionally added into the system in the form of a 5cm offset to one of the box dimensions. This had the effect of increasing the radius of the initial planned arc trajectory. As expected, the open loop approach always failed in this case. The single-modal closed loop approaches were still capable of completing full pivots in many cases, with success rates of 67.5-83.3%, despite high lift rates of 56.7-99.2%, corresponding to a frequent deviation from the ideal planned trajectory, but a recovery to complete the pivot. Out of all methods, the combined approach was the most robust, succeeding in all tests.

B. Effects of different objects

Mass: During our experiments, it was observed that the mass of the box could directly affect the success rate. For the force-based position and vision control methods performing short-to-long pivots, both the small box and the long box had 100% success rate while the large box had 50% only. The failed cases were caused by the low weight of the large box, which is the lightest out of all three boxes. This could not generate enough torque around the gripper fingers to induce rotational slip for the purpose of pivoting. Sufficient torque about the gripper fingers is necessary to create rotational slip as the the box is more capable of overcoming the friction force generated by the grasp. On the contrary, the long box showed a 0% success rate in terms of the pick&place method. During those experiments, the mass was the main reason for failure as the weight of the box cause too much slip for the robot to rotate the box 90°.

Object shape and Mass distribution: Besides the mass, the shape of the objects and their mass distributions also affect the gravitational torque around the gripper fingers. The long-to-short pivoting case has a higher torque than the short-to-long case, since the grasp point is further from the CoM, roughly at the center of the box. This helps to induce rotational slip at the grasp point and complete the pivot action. As seen in Table I-III, the success rates for the long-to-short pivots were generally higher for all methods, and the lift rates were

Small Box (Dimensions: $18 \times 11 \times 4$ cm, Weight: 1.27 kg)																					
		Short-to-Long Pivot								Long-to-Short Pivot											
		Without Noise				Added Noise				Without Noise				Added Noise							
		%	%	%	sec	J	%	%	%	sec	J	%	%	%	sec	J	%	%	%	sec	J
		Succ.	Lift	Slip	Time	Work	Succ.	Lift	Slip	Time	Work	Succ.	Lift	Slip	Time	Work	Succ.	Lift	Slip	Time	Work
Pick&Place		100	100	0	16.4	8.0	NA	NA	NA	NA	NA	100	100	0	18.2	8.0	NA	NA	NA	NA	NA
Open Loop		0	100	0	-	-	0	100	0	-	-	100	0	0	10.4	2.7	0	100	0	-	-
Vision		100	100	0	22.7	4.4	100	100	0	23.2	4.7	100	100	0	24.1	2.2	100	100	0	24.3	2.3
Gripper		100	0	0	27.0	1.6	0	100	0	-	-	100	0	0	29.6	1.9	0	90	10	-	-
Force		100	100	0	22.9	6.4	100	100	0	23.5	5.8	100	0	0	23.8	3.1	100	80	0	21.7	2.1
Gripper+Force+Vision		100	10	0	25.3	1.1	100	0	0	24.4	1.7	100	0	0	26.4	1.5	100	0	0	24.9	1.8

TABLE I: Small box experiment results summary.

Large Box (Dimensions: $23 \times 16 \times 5$ cm, Weight: 0.88 kg)																					
		Short-to-Long Pivot								Long-to-Short Pivot											
		Without Noise				Added Noise				Without Noise				Added Noise							
		%	%	%	sec	J	%	%	%	sec	J	%	%	%	sec	J	%	%	%	sec	J
		Succ.	Lift	Slip	Time	Work	Succ.	Lift	Slip	Time	Work	Succ.	Lift	Slip	Time	Work	Succ.	Lift	Slip	Time	Work
Pick&Place		100	100	0	16.1	6.6	NA	NA	NA	NA	NA	100	100	0	16.6	5.9	NA	NA	NA	NA	NA
Open Loop		0	100	0	-	-	0	100	0	-	-	70	0	0	10.8	4.0	0	100	0	-	-
Vision		0	100	0	-	-	0	100	0	-	-	100	90	0	24.4	5.5	100	100	0	28.1	3.1
Gripper		100	90	0	26.8	2.4	30	100	10	28.3	4.3	100	0	0	26.7	1.9	100	100	0	34.0	2.5
Force		0	100	0	-	-	0	100	0	-	-	100	0	0	24.4	5.4	100	80	0	25.1	3.3
Gripper+Force+Vision		100	0	0	25.5	1.8	100	0	0	25.8	1.9	100	0	0	26.2	2.3	100	0	0	26.9	1.9

TABLE II: Large Box experiment results summary.

Long Box (Dimensions: $28 \times 12 \times 5$ cm, Weight: 1.72 kg)																					
		Short-to-Long Pivot								Long-to-Short Pivot											
		Without Noise				Added Noise				Without Noise				Added Noise							
		%	%	%	sec	J	%	%	%	sec	J	%	%	%	sec	J	%	%	%	sec	J
		Succ.	Lift	Slip	Time	Work	Succ.	Lift	Slip	Time	Work	Succ.	Lift	Slip	Time	Work	Succ.	Lift	Slip	Time	Work
Pick&Place		0	100	0	-	-	NA	NA	NA	NA	NA	0	100	0	-	-	NA	NA	NA	NA	NA
Open Loop		90	10	0	9.3	8.7	0	100	0	-	-	100	0	0	10.8	12.7	0	100	0	-	-
Vision		100	100	0	24.6	4.1	100	100	0	28.2	4.0	100	100	0	28.7	5.3	100	100	0	31.0	5.2
Gripper		90	0	10	28.7	3.6	90	100	10	35.1	9.8	100	0	0	29.8	7.0	0	100	50	-	-
Force		100	0	0	23.9	4.5	100	100	0	24.9	4.9	100	0	0	26.1	7.1	100	0	0	27.4	4.8
Gripper+Force+Vision		100	0	0	29.3	2.9	100	0	0	30.4	3.3	100	0	0	30.6	3.9	100	0	0	33.1	3.7

TABLE III: Long box experiment results summary. ‘NA’ indicates no such cases were tested since no dimensions of the boxes are used in the pick&place method. ‘-’ is used for cases where the robot failed to do pivoting in all experiments.

	%	%	%	sec	J
	Succ.	Lift	Slip	Time	Work
Pick&Place	66.7	100	0	16.8	7.1
Open Loop	30	67.5	0	10.3	7.0
Vision	83.3	99.2	0	25.9	4.1
Gripper	67.5	56.7	7.5	29.6	3.9
Force	83.3	55	0	24.4	4.7
Force + Gripper + Vision	100	0	0	27.4	2.3

TABLE IV: Aggregate results from 60 trials for the Pick&Place method (Pick&Place was not run for the noisy dimension condition), and 120 for each of the other methods.

generally lower. This was especially significant for the single-modal approaches without gripper control, as they lack the means to regulate the extrinsic influence of gravitational torque by varying gripper width.

However, the iron weights used to manually adjust the weight of the boxes would not have been perfectly distributed around the center. Thus the torque around the fingers can be difficult to estimate, with variation in object weight, geometry and distribution.

C. Artificial Markers for Pose Estimation

In the vision component of our system, the ArUco marker plays an important role in detecting the object’s pose and further tracking the angle between the surface and the box’s lowest edge among all approaches. More generalizable methods for pose estimation may include point cloud clustering and feature matching in the 3D space [27]. Such algorithms can also be used to derive the dimensions of the object. Although this may introduce inaccuracies to the vision component, our tests have shown that by using closed loop approaches, the system can succeed in the face of such inaccuracies.

D. Single vs Multi-modal

In our combined approach, all three modules are necessary for the “perfect” pivoting. Based on the results in Table.IV, each single-modal controller was not able to pivot the box with 100% success rate.

Both vision and force-based position controllers have higher success rate than the gripper module, as our chosen challenge scenario introduced noise to the ideal arc trajectory, which could only be amended by the offsets produced by those two controllers. For some specific scenarios (i.e. light weight box),

the box can easily be lifted without inducing enough rotational slip, and the gripper controller can be more important to complete pivoting. In the case of vision control, the robot only begins to offset the trajectory after the box has been lifted, causing a high lift rate of 99.2%, and inducing some unnecessary motions.

VI. CONCLUSIONS AND FUTURE WORK

We present a closed loop, multi-modal solution utilising vision, force/torque and tactile sensors for manipulating objects via pivoting. The system is able to control the robot's end-effector trajectory to maintain contact with the surface, and modulate the gripper finger width to induce the desired type of slip.

Based on the experiments we conducted, we observe a clear advantage of our approach in terms of success rate, robustness, as well as the work done in pivoting the box compared to the open loop and pick-and-place method. The limitations of our approach are its slow execution speed, being significantly slower than the other two methods. For future works, we will consider implementing joint velocity control to reduce the time taken, as well as removing the use of markers for object detection and generalising this approach for many different shapes of objects. Additionally, using learning to perform force-based position and gripper width control will be considered.

This paper should be considered as a proof-of-concept that demonstrates the feasibility of our pivoting approach by taking advantage of multi-modal sensing. While our work featured only cubic objects tracked via fiducial markers, we believe that our approach can be generalized to rigid objects with modifications. The marker-based pose detection can be swapped with a model-based 6D pose detector [28]. A model-based [29] or model-free grasp synthesis approach [30] can be used for obtaining a robust 6D grasp pose. In our work, pivoting on an edge of the box was obvious, however, to generalize it to any given object, further geometric reasoning would be needed for finding a suitable pivot point or edge on the object. Furthermore, a more sophisticated control approach might be needed for contact configuration regulation [18].

REFERENCES

- [1] Y. Aiyama, M. Inaba, and H. Inoue, "Pivoting: A new method of graspless manipulation of object by robot fingers," in *IEEE/RSJ International Conference on Intelligent Robots and Systems (IROS)*, 1993.
- [2] S. Saeedvand, H. Mandala, and J. Baltes, "Hierarchical deep reinforcement learning to drag heavy objects by adult-sized humanoid robot," *Applied Soft Computing*, 2021.
- [3] N. C. Dafle, A. Rodriguez, R. Paolini, B. Tang, S. S. Srinivasa, M. Erdmann, M. T. Mason, I. Lundberg, H. Staab, and T. Fuhlbrigge, "Extrinsic dexterity: In-hand manipulation with external forces," in *IEEE International Conference on Robotics and Automation (ICRA)*, 2014.
- [4] M. Costanzo, G. De Maria, and C. Natale, "Slipping control algorithms for object manipulation with sensorized parallel grippers," in *IEEE International Conference on Robotics and Automation (ICRA)*, 2018.
- [5] T. M. Huh, H. Choi, S. Willcox, S. Moon, and M. R. Cutkosky, "Dynamically reconfigurable tactile sensor for robotic manipulation," *IEEE Robotics and Automation Letters*, 2020.
- [6] M. Meier, F. Patzelt, R. Haschke, and H. J. Ritter, "Tactile convolutional networks for online slip and rotation detection," in *International Conference on Artificial Neural Networks*, pp. 12–19, Springer, 2016.
- [7] J. Toskov, R. Newbury, M. Mukadam, D. Kulić, and A. Cosgun, "In-hand gravitational pivoting using tactile sensing," in *Conference on Robot Learning*, 2022.
- [8] M. Raessa, W. Wan, and K. Harada, "Planning to repose long and heavy objects considering a combination of regrasp and constrained drooping," *Assembly Automation*, vol. 41, no. 3, pp. 324–332, 2021.
- [9] A. Zhang, K. Koyama, W. Wan, and K. Harada, "Manipulation planning for large objects through pivoting, tumbling, and regrasping," *Applied Sciences*, vol. 11, no. 19, p. 9103, 2021.
- [10] F. Shi, M. Zhao, M. Murooka, K. Okada, and M. Inaba, "Aerial regrasping: Pivoting with transformable multilink aerial robot," in *IEEE International Conference on Robotics and Automation (ICRA)*, 2020.
- [11] E. Yoshida, M. Poirier, J.-P. Laumond, O. Kanoun, F. Lamiraux, R. Alami, and K. Yokoi, "Pivoting based manipulation by a humanoid robot," *Autonomous Robots*, vol. 28, no. 1, pp. 77–88, 2010.
- [12] R. Antonova, S. Cruciani, C. Smith, and D. Kragic, "Reinforcement learning for pivoting task," *arXiv preprint arXiv:1703.00472*, 2017.
- [13] Y. Hou, Z. Jia, and M. T. Mason, "Fast planning for 3d any-pose-reorienting using pivoting," in *2018 IEEE International Conference on Robotics and Automation (ICRA)*, pp. 1631–1638, IEEE, 2018.
- [14] Y. Hou, Z. Jia, and M. T. Mason, "Reorienting objects in 3d space using pivoting," *arXiv preprint arXiv:1912.02752*, 2019.
- [15] B. Siciliano and L. Villani, *Robot force control*. Springer Science & Business Media, 1999.
- [16] D. Ma, S. Dong, and A. Rodriguez, "Extrinsic contact sensing with relative-motion tracking from distributed tactile measurements," in *IEEE international conference on robotics and automation (ICRA)*, 2021.
- [17] A. Molchanov, O. Kroemer, Z. Su, and G. S. Sukhatme, "Contact localization on grasped objects using tactile sensing," in *IEEE/RSJ International Conference on Intelligent Robots and Systems (IROS)*, 2016.
- [18] N. Doshi, O. Taylor, and A. Rodriguez, "Manipulation of unknown objects via contact configuration regulation," in *IEEE International Conference on Robotics and Automation (ICRA)*, 2022.
- [19] F. R. Hogan, J. Ballester, S. Dong, and A. Rodriguez, "Tactile dexterity: Manipulation primitives with tactile feedback," in *IEEE International Conference on Robotics and Automation (ICRA)*, 2020.
- [20] K.-T. Yu and A. Rodriguez, "Realtime state estimation with tactile and visual sensing for inserting a suction-held object," in *IEEE/RSJ International Conference on Intelligent Robots and Systems (IROS)*, 2018.
- [21] Q. Li, O. Kroemer, Z. Su, F. F. Veiga, M. Kaboli, and H. J. Ritter, "A review of tactile information: Perception and action through touch," *IEEE Transactions on Robotics*, vol. 36, no. 6, pp. 1619–1634, 2020.
- [22] M. Costanzo, G. De Maria, and C. Natale, "Two-fingered in-hand object handling based on force/tactile feedback," *IEEE Transactions on Robotics*, vol. 36, no. 1, pp. 157–173, 2019.
- [23] M. Costanzo, G. De Maria, and C. Natale, "Detecting and controlling slip through estimation and control of the sliding velocity," *Applied Sciences*, vol. 13, no. 2, p. 921, 2023.
- [24] C. Wang, X. Zang, H. Zhang, H. Chen, Z. Lin, and J. Zhao, "Status identification and object in-hand reorientation using force/torque sensors," *IEEE Sensors Journal*, vol. 21, no. 18, pp. 20694–20703, 2021.
- [25] Y. Chen, C. Prepscius, D. Lee, and D. D. Lee, "Tactile velocity estimation for controlled in-grasp sliding," *IEEE Robotics and Automation Letters*, vol. 6, no. 2, pp. 1614–1621, 2021.
- [26] H. Khamis, R. I. Albero, M. Salerno, A. S. Idil, A. Loizou, and S. J. Redmond, "Papillarray: An incipient slip sensor for dexterous robotic or prosthetic manipulation—design and prototype validation," *Sensors and Actuators A: Physical*, vol. 270, pp. 195–204, 2018.
- [27] J. Guo, X. Xing, W. Quan, D.-M. Yan, Q. Gu, Y. Liu, and X. Zhang, "Efficient center voting for object detection and 6d pose estimation in 3d point cloud," *IEEE Transactions on Image Processing*, vol. 30, pp. 5072–5084, 2021.
- [28] Y. Xiang, T. Schmidt, V. Narayanan, and D. Fox, "Posecnn: A convolutional neural network for 6d object pose estimation in cluttered scenes," 2018.
- [29] J. Tremblay, T. To, B. Sundaralingam, Y. Xiang, D. Fox, and S. Birchfield, "Deep object pose estimation for semantic robotic grasping of household objects," in *Conference on Robot Learning (CoRL)*, 2018.
- [30] A. Mousavian, C. Eppner, and D. Fox, "6-dof grapsnet: Variational grasp generation for object manipulation," in *IEEE/CVF International Conference on Computer Vision (CVPR)*, 2019.